Time-of-flight study of bound exciton polariton dispersive propagation in ZnO

2005 J. Phys.: Condens. Matter 17 7287

(http://iopscience.iop.org/0953-8984/17/46/012)

INSTITUTE OF PHYSICS PUBLISHING JOURNAL OF PHYSICS: CONDENSED MATTER

J. Phys.: Condens. Matter **17** (2005) 7287–7296 doi:10.1088/0953-8984/17/46/012

Time-of-flight study of bound exciton polariton dispersive propagation in ZnO

Gang Xiong[1], John Wilkinson[2], K B Ucer and R T Williams

Department of Physics, Wake Forest University, Winston Salem, NC 27109-7507, USA

E-mail: gang.xiong@pnl.gov

Received 21 May 2005, in final form 3 October 2005
Published 1 November 2005
Online at stacks.iop.org/JPhysCM/17/7287

Abstract

We report direct observations of polariton dispersive propagation at the donor-bound exciton (D^0X) resonance in single-crystal ZnO. Time-resolved photoluminescence spectra are measured from both surfaces of a ZnO single crystal that is excited in a thin layer on one surface. When the excitation and the detector are at opposite sides of the crystal, the time-resolved luminescence spectrum in the streak camera display has a curved shape in the t versus $\hbar\omega$ plane, indicating dispersion in transport time across the crystal thickness. The group velocity at the donor-bound exciton resonance (3.36 eV) is measured to be 6×10^6 m s^{-1}. The EHP (electron–hole plasma) relaxation time is about 36 ps, in agreement with published results. The polariton reflection at the crystal boundary is observed in the time domain, confirming the dispersion hypothesis. The low-temperature transmission spectrum shows that optical emission from the donor-bound exciton polariton is attenuated by 95% on traversing 0.5 mm crystal thickness due to reflections and polariton decay. From these data the D^0X polariton lifetime is estimated as 37 ps. The temperature-dependent change of streak camera curvatures corresponds to thermal de-trapping of the donor-bound excitons.

(Some figures in this article are in colour only in the electronic version)

1. Introduction

Recent experimental [1, 2] and theoretical studies [3, 4] showed evidence of giant oscillator strength in ZnO exciton spectra, especially the neutral donor-bound exciton (D^0X), due to extended spatial coherence of the exciton states. In addition, the exciton binding energy of 60 meV in ZnO substantially exceeds kT at room temperature. Together these factors lead us

[1] Author to whom any correspondence should be addressed. Present address: Pacific Northwest National Laboratory, PO Box 999, K8-88, Richland, WA 99352, USA.

[2] Present address: Chemistry Division, Code 6125, Naval Research Laboratory, 4555 Overlook Avenue, SW Washington, DC 20375-5342, USA.

0953-8984/05/467287+10$30.00

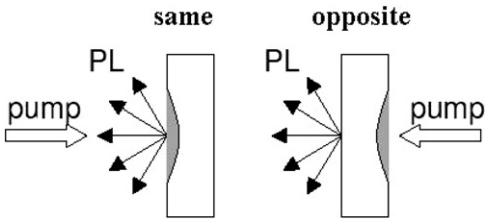

Figure 1. Measurements with the pump beam and detector at the same side are labelled as 'same', while measurements with the pump beam and detector at different sides of the crystal are 'opposite'. Both surfaces were polished the same.

to expect that photon–exciton coupling should be significant in near-edge optical properties of ZnO. Kavokin *et al* discussed the possibility of Bose condensation of exciton polaritons in ZnO and suggested ZnO as a material well adapted for the realization of a room-temperature polariton laser [5].

The propagation of a bound-exciton polariton can be understood as a long-range phased coherence of many localized (bound) excitons in the crystal. The radiation from the recombination of one local exciton is absorbed to form another localized exciton state, and that localized exciton state then re-emits a photon. The propagation of a bound-exciton polariton is realized by such absorption and re-emission processes, as discussed by Kavokin *et al* [6]. Although there have been a few studies [7–10] on the exciton polariton in ZnO, a time-of-flight study of polariton dispersion and propagation in ZnO has not been previously published. It is of interest to study the qualitative strength of photon–exciton coupling and energy dispersion in ZnO, and the polariton decay rate. In this paper, we report the direct observation of the ZnO donor-bound exciton polariton propagation, internal reflection at the crystal surface, and the energy dispersion curve by picosecond time-resolved photoluminescence spectroscopy. The donor-bound exciton polariton group velocity and EHP (electron–hole plasma) relaxation time are calculated. The polariton decay rate is calculated based on the percentage attenuation of polaritons propagating through the crystal. We will show that the results derived are self-consistent and fit relatively well with the results obtained by other methods [2, 11].

2. Experiment

Two pieces of ZnO single-crystal samples produced by Eagle-Picher Inc. were used in our experiments. The ZnO single crystals were grown by the seeded chemical vapour transport technique. The (0001) wafer surfaces were chemo-mechanically polished to epitaxy substrate standards by Eagle-Picher. The thicknesses of these two samples are 0.5 and 1 mm, respectively. The excitation pulse used for this experiment was the third harmonic (273 nm) of a mode-locked Ti:sapphire laser amplified at 10 Hz. The pulse width was $\sim$300 fs. The average laser irradiance was approximately 3 mW cm^{-2} and the peak irradiance was $\sim$1 GW cm^{-2}. The temporal and wavelength spectra of ZnO luminescence were captured by a streak camera (Hamamatsu C2830 temporal disperser). The temporal resolution of the streak camera was measured as $\pm$13 ps including trigger jitter. The two experiment geometries are shown in figure 1. Excitation and photoluminescence detection at the same side of the crystal surface is labelled as 'same', while excitation of one surface and detection of the photoluminescence through the sample is labelled as 'opposite'. In both cases the laser beam propagates parallel to the *c*-axis of the ZnO crystal ($\mathbf{k} \parallel \mathbf{c}$ and $\mathbf{E} \perp \mathbf{c}$). Our experimental geometries are similar to those of Ziebold *et al*, who used these two geometries to study the supersonic EHP expansion in GaAs [12].

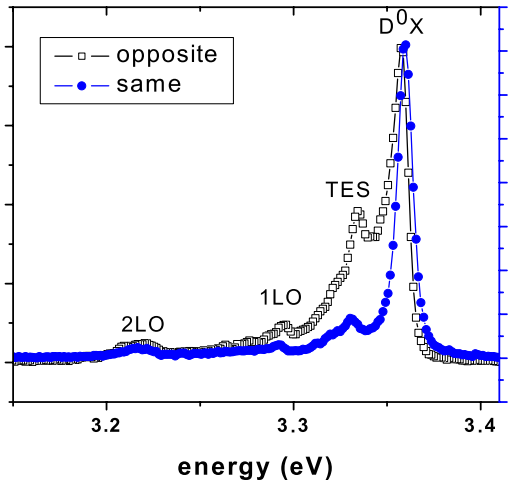

Figure 2. The luminescence spectra at 17 K. The luminescence intensities are normalized at the D^0X peak to make them equal in the 'same' and the 'opposite' geometries. Due to strong attenuation at the D^0X position, the actual D^0X peak of the 'opposite' spectrum is only 5% that of the 'same' spectrum.

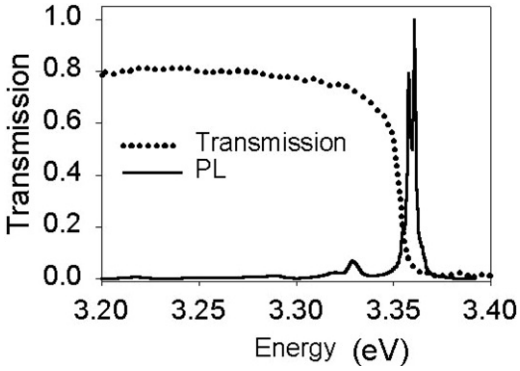

Figure 3. Optical transmission of the sample is overlaid on the 'same' spectrum of photoluminescence. Both were measured at 17 K. At the transparent region, only 70%–80% of light can transmit through the crystal, because the rest is reflected at the surfaces.

3. Time-resolved luminescence spectra at 17 K

The integrated luminescence spectra at 17 K from both 'opposite' and 'same' geometries are shown in figure 2. Both spectra consist of the D^0X peak at 3.36 eV, its two-electron satellite (TES) at 3.32 eV, and LO-phonon replicas at 3.29 and 3.22 eV, respectively. To show the similarity of both spectra in figure 2 we normalized them at the D^0X peak position. In fact the D^0X luminescence observed from the 'opposite' geometry is much weaker compared to that observed from the 'same' geometry. An *in situ* transmission experiment at 17 K shows that the intensity at the D^0X wavelength is strongly attenuated (nearly 95%) by transport across the 0.5 mm thick crystal (figure 3). The loss is caused both by absorption and by reflections at crystal boundaries as discussed later in equation (7).

The time-resolved photoluminescence spectra captured by the streak camera are shown in figure 4. The top spectral image was captured in the 'same' geometry, while the bottom one was in the 'opposite' geometry. The horizontal axis is the photon energy, while the vertical axis is the time. The full timescale is 550 ps. In both streak camera images, the most intense streaks located at 3.36 eV (between the cursor lines) are the D^0X luminescence peaks, while the weaker ones at 3.32 and 3.22 eV are the TES and second-order LO-phonon replicas ($D^0X + 2LO$), respectively. With background subtracted, the first-order LO-phonon replica ($D^0X + LO$) at 3.29 eV is measured to be approximately three times weaker than the

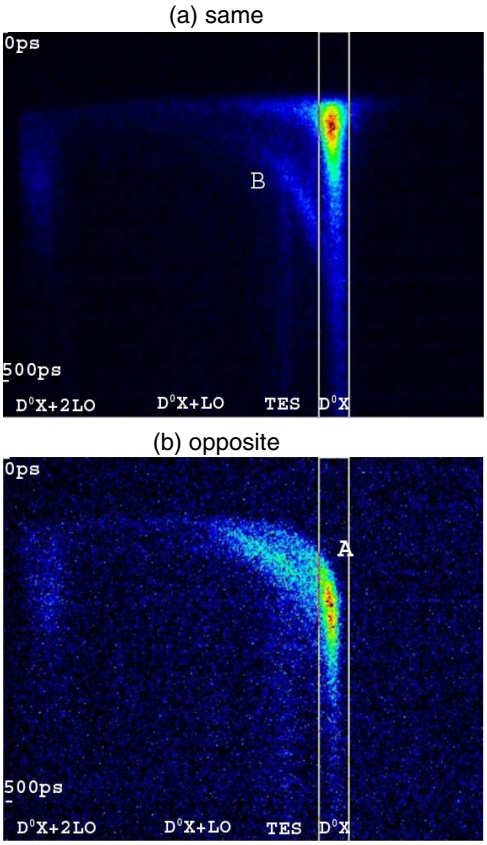

Figure 4. The time-resolved photoluminescence streaks in the $(t, \hbar\omega)$ plane measured at the 'same' and 'opposite' side relative to excitation. (Images are better rendered with pseudo-colour in the online publication.) (a) The 'same' geometry; (b) 'opposite' geometry. A similar but less intense curved streak can also be seen in (a), marked as 'B'. Comparing 'A' and 'B', one can find that the slope in streak 'B' is twice that in streak 'A', which indicates that the curvature in 'B' results from the internal reflection of light and transit of twice the crystal thickness.

second-order one ($D^0X + 2LO$), and is hardly seen in both streak camera images. It is not so surprising to find that the $D^0X + LO$ replica is weaker than the $D^0X + 2LO$ replica, as similar phenomena have been previously observed in some other semiconductor materials (see for example Permogorov [13] for a review and discussion). We have previously reported the $1/e$ lifetime of D^0X luminescence in ZnO as approximately 50 ps at 17 K [2]. The fast spontaneous radiative lifetime is attributed to the enhanced oscillator strength of a bound exciton coherent over its localization volume [4, 14, 15].

The most significant feature of the time-resolved photoluminescence spectra is the curvature of the $(t, \hbar\omega)$ streak in the 'opposite' geometry (marked as 'A' in figure 4(b)). The curvature indicates a spectral-dependent time delay of luminescence from the observed surface (figure 4(b)). The delay at 3.36 eV is 120 ps for a 0.5 mm thick crystal (as shown in figure 5), and 200 ps for a 1 mm thick crystal. Notice that a similar but less intense curved trace can also be found in the 'same' image (marked as 'B' in figure 4(a)). It has a slope twice as large as the curvature 'A' in the 'opposite' image, and correspondingly, the peak delay time is approximately twice as long as that in the 'opposite' image.

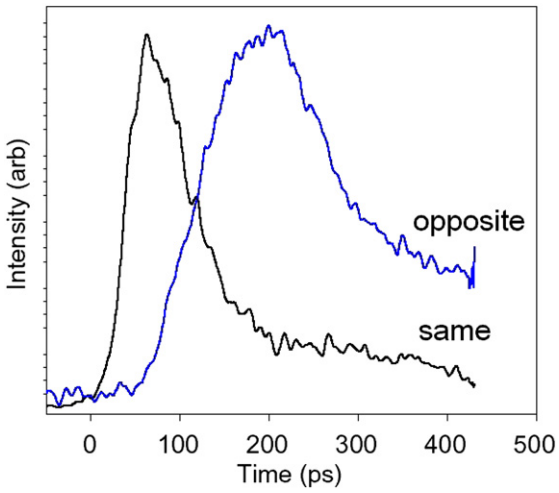

Figure 5. The time dependence of the PL intensity measured at 3.36 eV is compared for the 'same' and 'opposite' geometries for a 0.5 mm thick crystal.

3.1. Energy transport from one crystal surface to the other

The curvature of streak 'A' and the corresponding time delay for achieving peak intensity in the 'opposite' spectrum shows some kind of dispersive transport behaviour. According to the measured data of delay time, the energy transport velocity is in the range of 10^6 m s^{-1} (3×10^6 and 4.2×10^6 m s^{-1} respectively, if only a single mechanism is responsible for the delay).

One direct conclusion from the experimental results is that luminescence photons with different energy are either created at different times or travelling with different speeds, or both. The transport velocity is very slow compared to the speed of light in vacuum and typical 'transparent' materials. On the other hand, it is approximately two orders of magnitude faster than the speed of sound in a solid, which is believed to characterize typical expansion of EHP in GaAs [12], for example. By combining these two hypotheses together, and further considering the fact that the photons are near a bound exciton resonance of the crystal, a better hypothesis can be obtained. The exciton–photon coupling, which yields a substantially larger refractive index n, indicates a potentially much slower speed of light in the crystal. We attribute the time delay to the effect of two mechanisms, i.e., EHP expansion and polariton dispersion.

Our hypothesis is stated as following: with the incident above-band-gap laser pulse, an EHP is produced close to the pumped surface. Because of band gap renormalization, the optical emission of the plasma is shifted to a smaller energy compared to the band gap of the unexcited crystal comprising most of the transport path, so the light escapes easily. However, the EHP emission does not benefit from the oscillator strength enhancement that applies to D^0X [2], so light emission from the EHP is observed at considerably lower intensity in figure 4(a) than the bound exciton at 3.36 eV (and even in the 'opposite' geometry). In both cases the EHP intensity only presents itself as the spectral background since luminescence from the donor-bound exciton and its family of replicas dominates. As the plasma expands and undergoes Auger and radiative decay to lower density, the optical emission shifts toward higher energy, as observed in the upper beginning part of the curving streak in the 'opposite' view of figure 4(b). To give an idea of this timescale, the EHP relaxation time in ZnO thin-film material is 30 ps, as reported by Yamamoto, *et al* [11]. The 30 ps time delay caused by EHP expansion, however, is only a fraction of the total delay time (120 and 200 ps as given above) and cannot be solely responsible for the delay of energy transport.

We attribute the main part of the curving streak to dispersion of the donor-bound exciton polariton. The refractive index is a function of photon energy. When the photon energy is closely resonant with excitons, the photon–exciton coupling (exciton polariton) becomes strong. According to the lower branch of the polariton dispersion curve, the larger the photon energy, the smaller the polariton group velocity. Research on GaAs [16] and InI (indium iodide) [17] has shown that the exciton polariton propagation velocity is a few orders of magnitude smaller than the speed of light in vacuum.

The curvature 'B' in the 'same' streak camera image can then be understood (figure 4(a)). Since the slope in curvature 'B' is twice that of curvature 'A', and the corresponding delay time is approximately twice as long, it is concluded that the less intense curved streak 'B' results from the internal reflection of polaritons at the crystal boundary. The corresponding optical path length is therefore twice as long, which consequently yields a delay time and curvature slope twice as big.

Based on this hypothesis, the total delay time consists of the EHP relaxation time and the time it takes for the polariton to propagate through the crystal, as given in equation (1).

$$t_{\mathrm{delay}}(3.36\ \mathrm{eV}) = \tau_{\mathrm{EHP}} + \frac{d}{v_{\mathrm{g}}(3.36\ \mathrm{eV})}. \tag{1}$$

Given the experimental data from two samples of different thickness (120 ps for a 0.5 mm thick crystal, and 200 ps for a 1 mm thick crystal), we solve equation (1) for τ_{EHP} and $v_{\mathrm{g}}(3.36\ \mathrm{eV})$. The calculated EHP relaxation time and the polariton group velocity at 3.36 eV are:

$$\tau_{\mathrm{EHP}} = 36 \pm 13\ \mathrm{ps} \tag{2}$$

$$v_{\mathrm{g}}(3.36\ \mathrm{eV}) = (6 \pm 1) \times 10^{6}\ \mathrm{m\ s^{-1}}. \tag{3}$$

3.2. EHP relaxation

Our result of 36 ± 13 ps EHP relaxation time is close to the 30 ps measured in ZnO by Yamamoto *et al* [11]. To further prove that the EHP expansion partially contributes to the time delay and the curvature in 'opposite' geometry, we studied the power dependence of the time-resolved 'opposite' spectra as shown in figure 6. The luminescence spectra of the first 36 ps were integrated and are plotted by triangle symbols versus excitation intensity. Correspondingly, the integrated luminescence after 36 ps are plotted by square symbols.

The data points are then fitted to the excitation power relationship $I_{\mathrm{l}} = C I_{\mathrm{e}}^{\beta}$, where I_{l} is the intensity of luminescence, I_{e} is the intensity of excitation, and β is the power exponent. The results give $\beta = 1.37$ for luminescence of the first 36 ps, and $\beta = 0.5$ for luminescence thereafter. The different power dependences (super-linear and sub-linear, respectively) at different time regions indicate different luminescence mechanisms. It is known that super-linear power dependence is the characteristic of EHP luminescence, while the saturation of D^0X luminescence because of dilute defect involvement has previously been observed [18]. The power-dependence results further support our hypothesis of attributing the curvature and total delay time to the EHP relaxation followed by the polariton propagation.

3.3. Polariton dispersion

We now focus our attention on polariton dispersion. The time delays at different energies can be directly measured from the curving streak. After properly subtracting the delay time caused by EHP expansion, we can plot the polariton dispersion curve according to the following calculation.

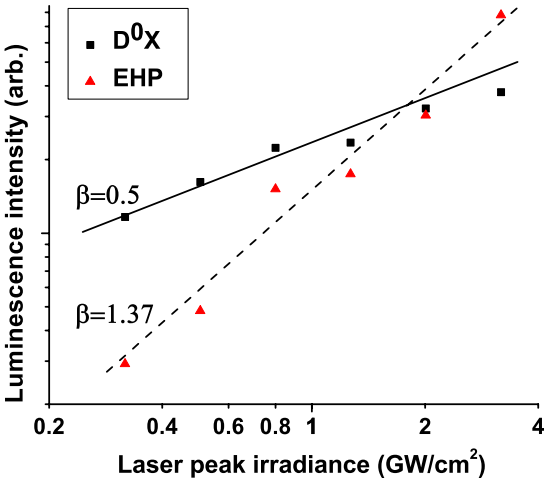

Figure 6. The log–log plots of the power dependence of luminescence. Triangle symbols: EHP luminescence integrated ($t < 36$ ps); square symbols: luminescence from D^0X and its family of replicas integrated ($t > 36$ ps).

The group velocity $v_g(k)$ is:

$$v_g(k) = \frac{dE(k)}{d(\hbar k)} \tag{4}$$

so:

$$k(E) = k(E_a) + \frac{1}{\hbar}\int_{E_a}^{E} \frac{1}{v_g(k)}\,dE$$
$$= k(E_a) + 15.15 \times 10^{14}\int_{E_a}^{E} \frac{1}{v_g(E)}\,dE \tag{5}$$

where E has the unit of electron volt, and k has the unit of m^{-1}. $k(E_a)$ is the photon wavevector at a reference energy $E(a)$. The group velocity $v_g(E)$ at different energies around E_a can be directly calculated according to the measured delay data.

Hu *et al* [19] fitted a Cauchy equation to the available refractive index data of ZnO in the visible region [20]. From this we can estimate the refractive index $n = 2.31$ at 373 nm, chosen because it lies within the streak camera spectral range of figure 4. The corresponding photon energy of 3.32 eV is thus the reference energy E_a in equation (5), chosen to be in a region of relatively flat dispersion.

With $k(3.32\ \text{eV}) = 3.9 \times 10^7\ \text{m}^{-1}$, equation (5) now becomes:

$$k(E) = 3.9 \times 10^7 + 15.15 \times 10^{14}\int_{3.32\ \text{eV}}^{E} \frac{1}{v_g(E)}\,dE. \tag{6}$$

We can therefore plot the experimental polariton dispersion curve as shown in figure 7.

The propagation velocity $v_g(k)$ at 3.36 eV can be calculated from the slope of the dispersion curve, which yields $4.8 \times 10^6\ \text{m s}^{-1}$, roughly consistent with $6 \times 10^6\ \text{m s}^{-1}$ determined above in the EHP + polariton hypothesis. According to equation (6), the inaccuracy of choosing the refractive index at $E_a = 3.32$ eV does not affect the value of calculated group velocity at any given energy.

The phase velocity and the refractive index near the band edge can be directly calculated from the polariton dispersion curve ($v_p = \omega/k$, and $n = c/v_p$). The phase velocity at 3.36 eV is found to be $9.1 \times 10^7\ \text{m s}^{-1}$, yielding the refractive index $n = 3.3$ at 3.36 eV.

The transmission of light through a crystal in the polariton spectral region suffers from absorption (polariton decay) and loss due to reflections at crystal boundaries. For a thick slab

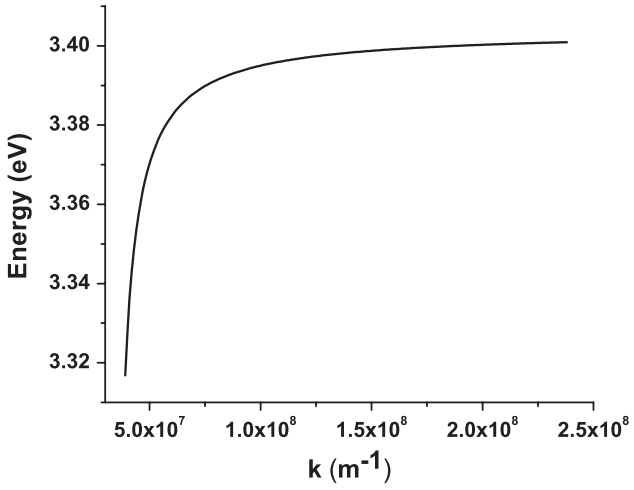

Figure 7. The measured polariton dispersion curve.

assuming no coherent interference, we can approximate the ratio of transmitted light by the following equation:

$$I_{\text{trans}}/I_0 = \sum_{m=1}^{+\infty}(1-R)^2 R^{2(m-1)}\,\mathrm{e}^{-(2m-1)\alpha d} = \frac{(1-R)^2\,\mathrm{e}^{-\alpha d}}{1-R^2\mathrm{e}^{-2\alpha d}} \tag{7}$$

where the reflectivity is:

$$R = |(n-1)/(n+1)|^2. \tag{8}$$

Here d is the thickness, and α the absorption coefficient. The reflectivity R at 3.36 eV is calculated as 0.29. Only approximately 5% of light (at 3.36 eV) can transmit through the crystal of 0.5 mm thickness. According to equation (7), the corresponding absorption coefficient can be calculated as 4.6 mm^{-1}.[3] It is worth noticing that the first partial transmitted ray is given by the numerator of equation (7), while the denominator effectively acts as a correcting factor to include multiple reflections. With $\alpha = 4.6\ \text{mm}^{-1}$, this correction comes out as 0.999, suggesting that only 0.1% of the contribution comes from higher-order partially transmitted rays.

Since we already know that the transit time across the 0.5 mm thick crystal at 3.36 eV is 84 ps (120 − 36 = 84 ps) for a 0.5 mm thick crystal, the polariton decay time can be estimated from the decay length. The corresponding polariton decay time (defined as the time taken for $1/e$ amount of polaritons to remain) is 37 ps, compared to our previous directly measured 50 ps lifetime of the donor-bound exciton [2]. Part of this difference results from the limited temporal resolution of the streak camera (±13 ps). In addition, the above treatment of transmission does not take the exciton spatial dispersion effect of ZnO into account [21]. The exciton spatial dispersion results in two transverse propagating waves in the bulk crystal, thus

[3] To be more accurate, when calculating the reflectivity using equation (8), n refers to the complex refractive index. Nevertheless, even near the resonance, the imaginary part (n_{i}) of the refractive indices of dielectric materials is in general much smaller than the real part (n_{r}), and much smaller than the imaginary refractive indices of metals, too. So the real part of n is a good approximation. To verify this, our calculated absorption coefficient ($\alpha = 4.6\ \text{mm}^{-1}$) can be used to roughly determine n_{i} by using the relation $n_{\text{i}} = \lambda_0\alpha/(2\pi)$ (where λ_0 is the photon wavelength in vacuum). The result gives n_{i} to be 2.7×10^{-4} compared to the real part ($n_{\text{r}} = 3.3$).

an additional boundary condition (ABC) is required to solve for the reflection coefficient [22]. Therefore equation (7) can only be regarded as a classical approximation and n represents the effective index of refraction.

4. Temperature dependence of polariton dispersion

We have previously measured the temperature evolution of ZnO luminescence spectra [23]. At 17 K, the D^0X replica dominates the PL spectra. As the temperature rises, the D^0X replica starts to thermally de-trap, and the 'free exciton' (FE) peak at 3.23 eV gradually becomes more important and dominates the spectrum at temperature above 100 K. (The 'free exciton' luminescence, as the 3.23 eV peak is commonly called, is the phonon-assisted A-exciton recombination transition.) At 293 K, the FE peak is at 3.26 eV and is broad and asymmetric, consisting mainly of the first-order (FE + LO) and the second-order (FE + 2LO) LO-phonon replicas.

In summary, the D^0X resonance responsible for the dispersion plotted in figure (polariton dispersion curve) is almost nonexistent above 100 K because the bound excitons are thermally de-trapped. The untrapped excitons determine the (temperature-dependent) dispersion around the 3.23 eV transition energy of the phonon-assisted free exciton resonance. A corresponding resonance behaviour in dispersion at this energy and temperature should be broader and weaker than at the D^0X peak (at lower temperature) because

(1) the composite peak of phonon-assisted transitions is spectrally much broader than the D^0X peak;
(2) the absorption coefficient at the peak of the D^0X transition is large due to its narrow width; and
(3) furthermore, the oscillator strength of the D^0X transition is dramatically enhanced by coherence of the bound exciton (giant oscillator strength) as discussed by Rashba [14], Henry and Nassau [15], and others [4].

When D^0X disappears due to the de-trapping of the exciton above 100 K, one can expect to lose the strong dispersive behaviour of exciton luminescence exhibited in figure 4 (streak camera images at 17 K).

A series of time-resolved spectra from the 'opposite' geometry from 16 to 293 K are plotted in figure 8. As the whole spectrum shifts to the lower energy position due to de-trapping of D^0X and also the narrowing of the band gap, the curvature becomes less significant, as expected from the discussion just above.

5. Conclusion

In summary, we have directly observed the exciton–polariton dispersion of transport time in ZnO. The donor-bound exciton polariton dispersion curve is plotted. According to the dispersion curve, the refractive indices near the band edge can be derived. The corresponding polariton propagation group velocity was measured as $(6 \pm 1) \times 10^6$ m s^{-1} at 3.36 eV, 50 times slower than the speed of light in vacuum.

Within a model that includes both EHP relaxation and polariton transport, our experiment yields the EHP relaxation time as 36 ± 13 ps. The excitation power dependence of luminescence and the temperature evolution of the streak camera spectra further support this assignment. The reflection of the polariton at the crystal surface was also observed to give a distinct echo dispersion (figure 4(a)).

The reflection coefficient at the D^0X resonance is calculated to be 0.29. The ratio of light transmitted through the crystal is evaluated based on a double-interface model taking

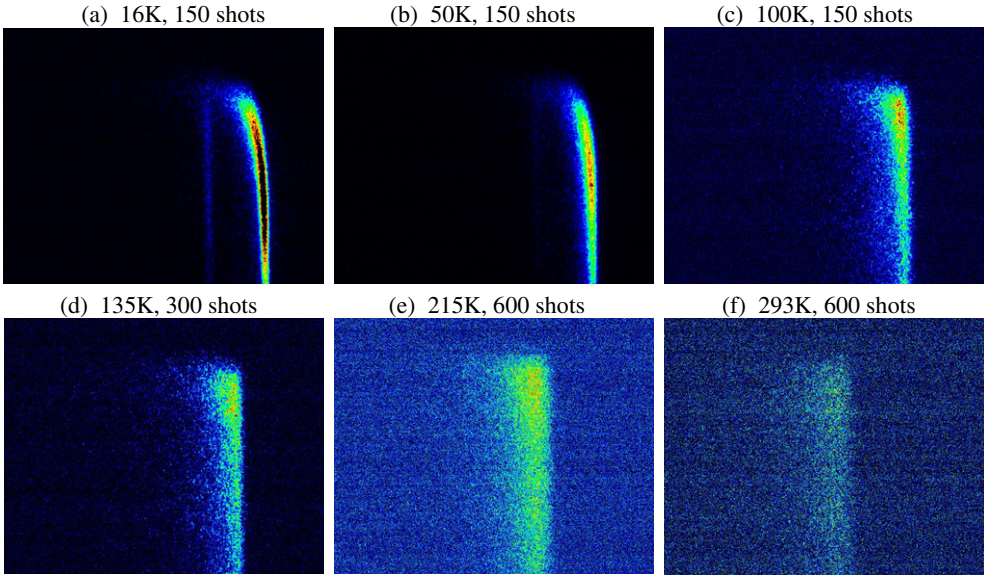

Figure 8. The temperature evolution of time-resolved photoluminescence spectra observed at the 'opposite' geometry.

multiple reflections and absorption into account. The resulting absorption coefficient at the D^0X wavelength is 4.6 mm^{-1}, from which an exciton polariton decay time of about 37 ps is estimated within the classical polariton picture.

References

[1] Zu P, Tang Z K, Wong G K L, Kawasaki M, Ohtomo A, Koinuma H and Segawa Y 1997 *Solid State Commun.* **103** 459
[2] Wilkinson J, Ucer K B and Williams R T 2004 *Radiat. Meas.* **38** 501
[3] Gil B and Kavokin A V 2002 *Appl. Phys. Lett.* **81** 748
[4] Xiong G, Wilkinson J, Ucer K B and Williams R T 2005 *J. Lumin.* **112** 1
[5] Kavokin A, Zamfirescu M, Gil B and Malpuech G 2003 *Phys. Status Solidi* a **192** 212
[6] Kavokin A V, Malpuech G and Langbein W 2001 *Solid State Commun.* **120** 259
[7] McGlynn E, Fryar J, Henry M O, Mosnier J P, Lunney J G, O' Mahony D and dePosada E 2003 *Physica* B **340** 230
[8] Reynolds D C, Look D C, Jogai B and Collins T C 2001 *Appl. Phys. Lett.* **79** 3794
[9] Chichibu S F, Sota T, Fons P J, Ivata K, Yamada A, Matsubara K and Niki S 2002 *Japan. J. Appl. Phys.* II **41** L935
[10] Wrzesinski J and Frohlich D 1997 *Phys. Rev.* B **56** 13087
[11] Yamamoto A, Kido T, Goto Y F, Chen Y, Yao T and Kasuya A 1999 *Appl. Phys. Lett.* **75** 469
[12] Ziebold R, Witte T, Hubner M and Ulbrich R 2000 *Phys. Rev.* B **61** 16610
[13] Permogorov S 1982 *Excitons* (Amsterdam: North-Holland) chapter 5, p 188
[14] Rashba E I and Guigenishvili G E 1962 *Sov. Phys.—Solid State* **4** 759
[15] Henry C H and Nassau K 1970 *Phys. Rev.* B **1** 1628
[16] Ogawa K, Katsuyama T and Nakamura H 1988 *Appl. Phys. Lett.* **53** 1077
[17] Jin F, Itoh T and Goto T 1989 *Japan. J. Phys. Soc.* **58** 2586
[18] Wilkinson J 2003 *PhD Dissertation* Wake Forest University, Winston Salem, NC 27109, USA
[19] Hu W S, Liu Z G, Sun J, Zhu S N, Xu Q Q, Feng D and Ji Z M 1997 *J. Phys. Chem. Solids* **58** 853
[20] Bond W L 1965 *J. Appl. Phys.* **36** 1674
[21] Skettrup T 1981 *J. Phys. D: Appl. Phys.* **14** 1343
[22] Hopfield J J and Thomas D G 1963 *Phys. Rev.* **132** 563
[23] Wilkinson J, Xiong G, Ucer K B and Williams R T 2002 *Nonlinear Opt.* **29** 529